

Understanding Crashback in Marine Propellers Using an Unsteady Actuator Disk Model

Martin Vyšohlíd* and Krishnan Mahesh†
University of Minnesota, Minneapolis, MN 55455

An unsteady actuator disk model is constructed in order to understand unsteadiness in crashback operation of a marine propeller as a competition between two flows of opposite direction: reversed flow through the propeller and the ambient flow due to motion of the vessel. The large eddy simulation methodology is applied to predict the flow corresponding to forward and crashback modes of operation using a non-dissipative, robust numerical algorithm developed by Mahesh et al. (2004, *J. Comput. Phys.*, 197: 215-240) for unstructured grids. Flow visualization shows creation and shedding of unsteady ring vortices which are correlated to the fluctuation of the thrust coefficient. Results of the model are compared to the LES of the full propeller geometry as well as to experimental data.

I. Introduction

CRASHBACK is an extreme operating condition for marine propulsors that often determines propulsor strength, and strongly affects overall maneuverability. In crashback the vessel is moving forward while the propeller rotates in reverse, so as to slow down the vessel. The flow around the propeller during crashback is characterized by massive separation, and large-scale unsteadiness. A prominent feature of the flow is an unsteady ring-vortex in the vicinity of the propeller disk. Jiang et al.¹ performed experiments of propeller crashback which provide PIV data on the ring-vortex. Detailed experiments which measure flow velocity in crashback using PIV and LDV were recently performed by Jessup et al.²

The unsteady Reynolds-averaged Navier-Stokes equations (RANS) represent the state-of-the-art in computational prediction of the viscous flow around propellers³⁻⁵. RANS appears capable of predicting forward mode and backing; however, significant disagreement with data is observed in crashback and crashahead conditions. Correct values of thrust and torque in crashback were predicted only recently by large eddy simulation (LES) of Vyšohlíd and Mahesh⁶. Results for one of their test cases is in Figure 1 for illustration. Figure 1a) shows contours and streamlines of instantaneous axial velocity in a cross-section passing through the propeller axis. Free stream flow is from left to right, the propeller is pushing water from right to left which creates recirculation region in the shape of a ring vortex. The flow and the ring vortex are highly irregular and unsteady. This leads to unsteady performance of the propeller as documented in Figure 1b), which shows evolution of non-dimensionalized thrust. Notice the low frequency fluctuations with a large amplitude, which are believed to be related to the behavior of the ring vortex.

The unsteadiness in propeller crashback comes from two different sources: 1) The competition between two flows of opposite directions: the reversed flow through the propeller and the ambient flow due to the motion of the vessel. 2) The fact that the propeller operates in the local unsteady flow in reverse, which means that the roles of leading and trailing edges of each blade are reversed. The local flow sees the sharp edge as leading edge and the thicker edge as trailing edge.

The goal of this paper is to understand the role of the first source of unsteadiness: the competition between two flows of opposite directions. The propeller is approximated by an actuator disk. As a consequence there is no distinction between forward operation of propeller and backing, and no distinction between crashback and crashahead in this model. Actuator disk approximations have been used earlier for simplified model of forward propeller operation by Rankine⁷, Froude⁸ and others. The classical derivation of actuator disk model assumes that pressure and velocity are uniform across the disk and constant in time. A streamtube passing through the propeller disk is considered and momentum and energy balance together with Bernoulli equation is used. A newer, more

* Graduate Research Assistant, Aerospace Engineering & Mechanics, AIAA student member

† Associate Professor, Aerospace Engineering & Mechanics, AIAA member

rigorous derivation by Spalart⁹ uses larger domain for momentum and energy balance and asymptotic solution of flow. He showed that if uniform pressure drop is assumed then velocity across the disk cannot be uniform. Both derivations assume that the flow is steady and inviscid and that there is a well defined streamtube leaving propeller disk in one direction. While these assumptions are reasonable in forward mode, they cannot be made in the crashback mode of operation. In crashback we want to get unsteady pressure on the propeller disk which leads to unsteady thrust. We assume constant velocity through the actuator disk and we solve the 3 dimensional, viscous, unsteady evolution of the flow using LES, which will allow us to compute the variable load of the actuator disk observed in crashback.

A similar problem as crashback appears in helicopter aerodynamics during so called vortex ring state of the rotor in vertical flight (see e.g. Leishman¹⁰), except that the rotor of a helicopter always rotates in the same direction, so the roles of leading and trailing edges are not reversed. The vortex ring state of a helicopter is equivalent to crashback in marine propellers, but our actuator disk model does not distinguish between crashback and crashahead.

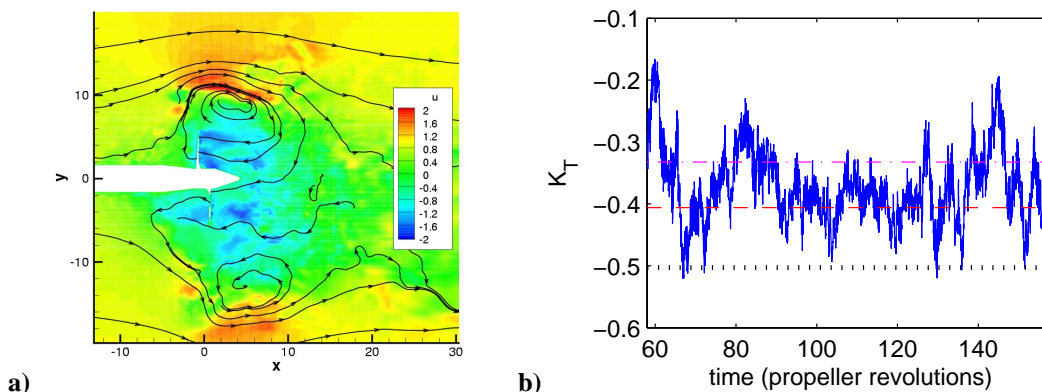


Figure 1: Results computed for real propeller geometry.⁶ (a) Side view of propeller. Contours show axial velocity normalized by U and streamlines for crashback $J = -0.7$, $Re = 480,000$, (b) time evolution of non-dimensionalized thrust: solid blue line is computed, dashed and dotted lines are mean values of three different experiments.

The paper is organized as follows. Section II describes the unsteady actuator disk model, section III briefly describes the numerical method and the computational grid. Results from the computations are shown in section IV. First, comparison of simulations corresponding to different modes of operation is presented (section IV.A), then the detail discussion of the ring vortex behavior in crashback and its correlation to thrust oscillation is discussed (section IV.B), followed by discussion of the effect of grid and a comparison with ring vortex behavior in crashback of the real propeller. A brief summary in section V concludes the paper.

II. Model description

The flow is described by incompressible Navier-Stokes equations:

$$\frac{\partial u_i}{\partial t} + \frac{\partial}{\partial x_j} (u_i u_j) = -\frac{\partial p}{\partial x_i} + \nu \frac{\partial^2 u_i}{\partial x_j \partial x_j},$$

$$\frac{\partial u_i}{\partial x_i} = 0$$

where u_i is the inertial velocity, p is the pressure, x_i are coordinates, t is time and ν is the kinematic viscosity. Note that the density is absorbed in pressure and the Einstein summation convention is used.

The propeller is approximated by a thin actuator disk with the same diameter as the real propeller which enforces constant flow velocity through the disk U_p parallel to the free-stream flow. Positive or negative value of U_p

correspond to the flow in the same or opposite direction as the free-stream flow, respectively. The domain of solution is a cylinder minus the actuator disk, see Figure 2, hence the constant velocity U_p is the boundary condition on the internal boundary of the domain. The boundary condition at the upstream face and the outer cylindrical surface is the constant free-stream velocity U , the downstream face has outflow boundary condition.

From the flow solution, thrust T can be obtained as the force of fluid acting on the actuator disk surface. Non-dimensional thrust K_T is then given by

$$K_T = \frac{T}{\rho n^2 D^4}$$

where ρ is the fluid density, n is a rotational speed in rev/s of the corresponding propeller and D is the diameter of the propeller/disk. This means that in order to model a real propeller, the disk velocity U_p needs to be set to average flow velocity through the real propeller and then this propeller rotational speed n should be used to evaluate K_T .

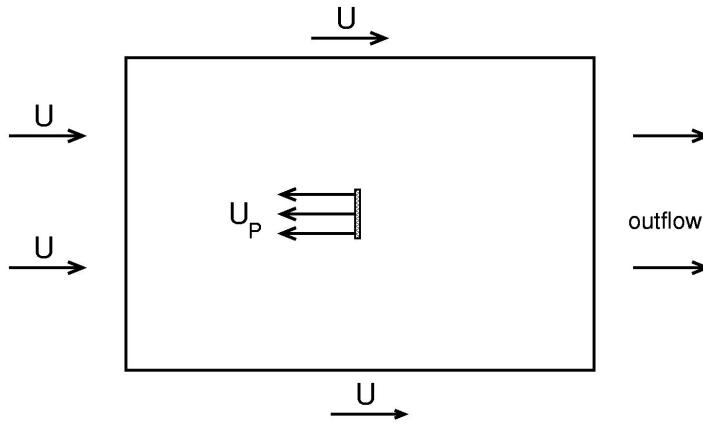


Figure 2: Schematics of actuator disk model of propeller.

III. Simulation details

The LES equations are obtained by spatially filtering (denoted by overbar) the Navier-Stokes equations. The filter is assumed to commute with the spatial and temporal derivatives. Applying the filter we get

$$\frac{\partial \bar{u}_i}{\partial t} + \frac{\partial}{\partial x_j} (\bar{u}_i \bar{u}_j) = -\frac{\partial \bar{p}}{\partial x_i} + \nu \frac{\partial^2 \bar{u}_i}{\partial x_j \partial x_j} - \frac{\partial \tau_{ij}}{\partial x_j},$$

$$\frac{\partial \bar{u}_i}{\partial x_i} = 0$$

where

$$\tau_{ij} = \overline{u_i u_j} - \bar{u}_i \bar{u}_j$$

is the subgrid stress and is modeled. The dynamic Smagorinski model as proposed by Germano et al.¹¹ and modified by Lilly¹² is used to model the subgrid stress.

The above equations are solved using a numerical method developed by Mahesh et al.¹³ for incompressible flows on unstructured grids. The algorithm is derived to be robust without numerical dissipation. It is a finite-volume approach which stores the Cartesian velocities and the pressure at the centroids of the cells (control volumes) and the face normal velocities are stored independently at the centroids of the faces. A predictor-corrector approach is used. The predicted velocities at the control volume centroids are first obtained and then interpolated to obtain the face-normal velocities. The predicted face normal velocity is projected so that continuity is discretely satisfied. This yields a Poisson equation for pressure which is solved iteratively using a multigrid approach. The pressure field is

used to update the Cartesian control volume velocities using a least-squares formulation. Time advancement is implicit and is performed using the Crank-Nicholson scheme. The algorithm has been validated for a variety of problems¹³ over a range of Reynolds numbers.

The computation was performed on a mesh with size of approximately 1 million control volumes. A commercial grid generator (Gambit & TGrid, Fluent Corporation) was used for the grid generation. The computational domain has diameter 7.3 times the propeller diameter and length 13.75 times the propeller diameter. The size of the domain was chosen to match the diameter of the widest part of the water tunnel used in experiments of Jessup et al. which is also the size used by Vyšohlíd and Mahesh⁶.

IV. Results

A. Modes of operation

Streamlines and contours of axial velocity for four different values of parameter U_p / U are shown in Figure 3. $U_p / U = 0.5$ in Figure 3a) corresponds to forward operation of propeller. The flow accelerates as it passes through the disk and the solution looks similar to that of a jet in a strong co-flow. Figure 3b) shows the solution for $U_p / U = 0.5$. Here the flow decelerates as it passes through the disk. There is a region of slightly accelerated flow around the disk as the decrease of velocity through the disk creates a constraint, but the flow still remains without large recirculation zones. This changes in Figure 3c), which shows solution for $U_p / U = 0$ where the disk acts as a bluff body with irregular recirculation zones downstream of the disk. Still in all cases in Figures 3a), 3b) and 3c) the fluctuation of thrust is small.

Figure 3d) shows solution for $U_p / U = -1$ which corresponds to the propeller crashback. In this case a recirculation zone in shape of a ring vortex is created which significantly influences the flow both downstream and upstream of the disk. In this case the fluctuation of thrust is much larger, similar as in the case of propeller crashback. The parameter $U_p / U = -1$ was chosen so that the flow through the disk resembles the flow around real propeller P4381 at advance ratio $J = -0.7$ used in experimental study² and in LES computation⁶, whose results are reproduced in Figure 1. Notice the reverse flow through the propeller and the ring vortex in Figure 1 similar to the actuator disk result in Figure 3d). Comparison of thrusts is in Table 1. Note that the results for real propeller geometry are for $Re \geq 480,000$ while the actuator disk result was computed only for $Re = 1,200$ and the ratio U_p / U matches the flow in real propeller only approximately. Despite of that, the disk model gives similar magnitude of thrust as real propeller in crashback.

B. Ring vortex behavior and thrust fluctuations

The pressure at the center of a vortex is lower, therefore the ring vortex can be visualized in 3-D by plotting the regions of low pressure. Figure 4 shows evolution of ring vortices computed by actuator disk model in time. Contours of axial velocity are plotted on surfaces corresponding to a small constant pressure. Note that the axial velocity inside the ring vortices is negative – opposite to free stream, while the axial velocity outside of the rings is positive and larger than free stream. This illustrates the flow circulation in ring vortices.

Changes in position, strength and shape of ring vortices affect the flow in the neighborhood of the propeller and therefore also the thrust. Non-dimensional thrust is plotted in Figure 5. The narrow peaks of thrust (i.e. narrow local minima of thrust magnitude, because thrust is negative) correspond to shedding of ring vortices. Arrows marked a), b), c) and d) show thrust values at times corresponding to plots with the same letter in Figure 4.

Figure 4a) shows a new ring vortex (right) created around the actuator disk (not shown) while the old ring vortex (left) drifts away with the free stream flow (from right top to left bottom corner) combined with self induced velocity. The magnitude of thrust is maximal at this time. Then it drops as the ring vortex develops and then slowly increases again as the ring vortex grows and gets further from the actuator disk as in Figure 4b). After it grows larger it starts stretching with one point attached close to the actuator disk as in Figure 4c) which corresponds to local maximum of thrust magnitude. Finally, the ring detaches as in Figure 4d) which corresponds to the narrow local minimum of thrust magnitude and the irregular cycle starts again.

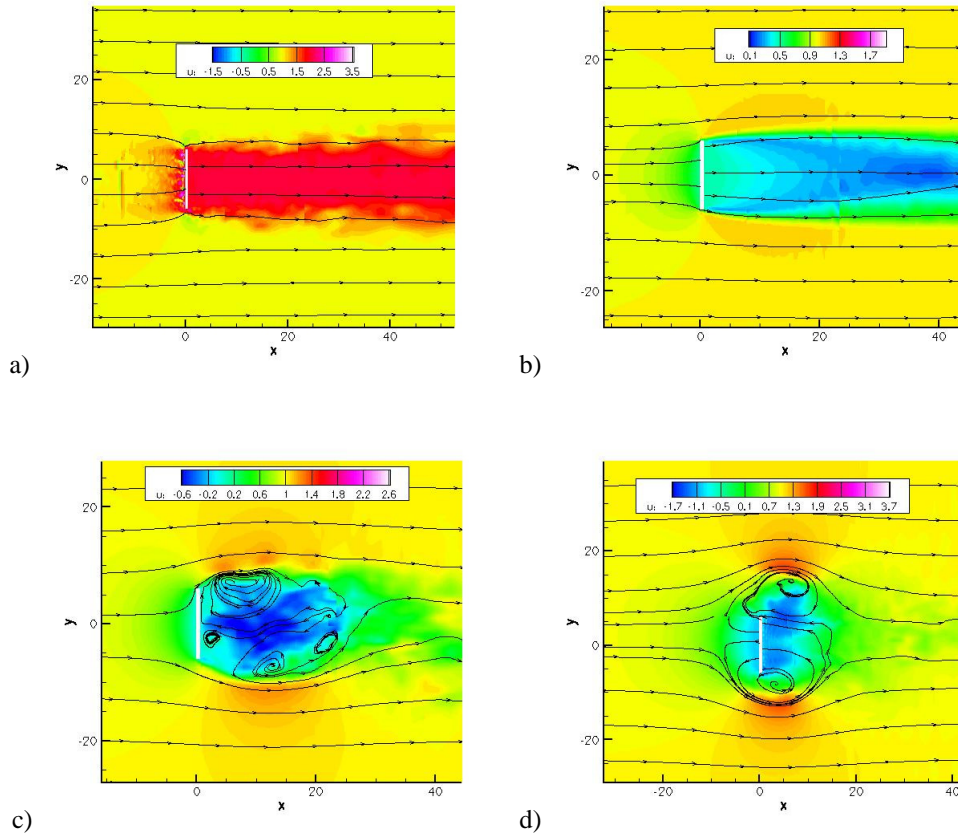


Figure 3: Computed streamlines and contours of axial velocity for results for actuator disk at $Re=1200$ and (a) $U_p/U=2$, (b) $U_p/U=0.5$, (c) $U_p/U=0$, (d) $U_p/U=-1$.

Table 1: Non-dimensional thrust K_T in crashback measured in experiments and computed for real propeller geometry at advance ratio $J = -0.7$ compared to actuator disk result for $U_p/U=-1$ and low $Re=1200$. All experimental data, including Hecker & Remmers¹⁴, were kindly provided by Jessup (private communication).

Crashback	J	K_T
Tow-tank, Hecker & Remmers [14]	-0.7	-0.5030
Tow-tank, Jessup (data 11/2004)	-0.7	-0.4062
Water tunnel, Jessup (data 9/2004)	-0.699	-0.3323
Computed for real propeller [6]	-0.7	-0.37
Computed for actuator disk ($U_p/U=-1$)	N / A	-0.6

The computation was done on a coarse grid of 1 million of control volumes. In order to verify the results, the mode $U_p / U = -1$, corresponding to crashback, was recomputed on a finer grid of 13 million of control volumes. The evolution of thrust computed on the fine grid is plotted in Figure 6. The fluctuations are more regular than on coarse grid (Figure 5), but both cases show low frequency fluctuations with similar period, mean value and amplitude. Both cases also show sharp peaks (short local minima of thrust), corresponding to ring vortex shedding and low slope peaks corresponding to growth of ring vortices.

The same visualization of the ring vortex was performed for the LES results of Vyšohlíd and Mahesh⁶ which compute flow around the real propeller. A typical plot is shown from two views in Figure 7. The evolution of the ring vortex in time does not show shedding of the whole ring vortex as was observed in the disk model. Instead only partial vortices leave the ring vortex and the relationship between thrust fluctuation and the ring vortex evolution is more complicated.

Conclusions

An unsteady actuator disk model was developed and the flow was computed for several values of model parameters. The model shows only small fluctuation of thrust in forward mode and large fluctuation of thrust in crashback in agreement with the real propeller simulation. The fluctuation of thrust in crashback is much larger than the fluctuation of drag force on a bluff body. The value of thrust predicted by the model is in similar range as that of the real propeller.

The unsteady actuator disk model shows presence of highly unsteady ring vortex and thrust similarly as in real propeller problem. The fluctuations of thrust in the unsteady actuator disk model are related to the cycle of the creation, growth, stretching and detachment of the ring vortex. The correspondence between thrust and ring vortex behavior is not so straightforward in case of the real propeller when the ring is not shed as whole but only partial vortices leave the ring vortex.

Acknowledgements

This work was supported by the United States Office of Naval Research under ONR Grant N00014-02-1-0978. Computing resources were provided by the San Diego Supercomputing Center, the National Center for Supercomputing Applications, and the Minnesota Supercomputing Institute. We are grateful to Dr. Stuart Jessup for providing us with experimental data, and for useful discussions.

References

- ¹Jiang, C.-W., Dong, R. R., Liu, H.-L., Chang, M.-S., "24-inch Water Tunnel Flow Field Measurements During Propeller Crashback," *21st Symposium on Naval Hydrodynamics*, The National Academies Press, Washington, DC, 1997, pp. 136-146.
- ²Jessup, S., Chesnakas, C., Fry, D., Donnelly, M., Black, S., Park, J., "Propeller Performance at Extreme off Design Conditions," *25th Symposium on Naval Hydrodynamics*, The National Academies Press, Washington DC, 2004, pp. 270-292.
- ³Chen, B., Stern, F., "Computational Fluid Dynamics of Four-Quadrant Marine-Propulsor Flow," *Journal of Ship Research*, Vol. 43, No. 4, 1999, pp. 218-228.
- ⁴Davoudzadeh, F., Taylor, L. K., Zierke, W. C., Dreyer, J. J., McDonald, H., Whitfield, D. L., "Coupled Navier-Stokes and Equations of Motion Simulation of Submarine Maneuvers, Including Crashback," *Proceedings of the 1997 ASME Fluids Engineering Division Summer Meeting*, Vol. 2, ASME, New York, 1997.
- ⁵McDonald, H., Whitfield, D., "Self-Propelled Maneuvering Underwater Vehicles," *21st Symposium on Naval Hydrodynamics*, The National Academic Press, Washington, DC, 1996, pp. 478-489.
- ⁶Vyšohlíd, M., Mahesh, K., "Large Eddy Simulation of Crashback in Marine Propellers," *AIAA Paper* 2006-1415.
- ⁷Rankine, W. J., "On the mechanical principles of the action of propellers," *Transactions of the Institute of Naval Architects* 6, 1865, pp. 13-39.
- ⁸Froude, R. E., "On the part played in propulsion by differences of fluid pressure," *Transactions of the Institute of Naval Architects* 30, 1889, pp. 390.
- ⁹Spalart, P. R., "On the simple actuator disk," *Journal of Fluid mechanics* 494, 2003, pp. 399-405.
- ¹⁰Leishman, J.G., "Principles of helicopter aerodynamics." Cambridge University Press, New York, 2000.
- ¹¹Germano, M., Piomelli, U., Moin, P., Cabot, W. H., "A Dynamic Subgrid-Scale Eddy Viscosity Model," *Physics of Fluids A*, Vol. 3, No. 7, 1991, 1760-1765.
- ¹²Lilly, D. K., "A Proposed Modification of the Germano Subgrid-Scale Closure Method", *Physics of Fluids A*, Vol. 4, No. 3, 1992, 633-635.
- ¹³Mahesh, K., Constantinescu, G., Moin, P., "A Numerical Method for Large-Eddy Simulation in Complex Geometries," *Journal of Computational Physics*, Vol. 197, No. 1, 2004, 215-240.
- ¹⁴Hecker, R., Remmers, K., "Four Quadrant Open-Water Performance of Propellers 3710, 4024, 4086, 4381, 4382, 4383, 4384 and 4426," David Taylor Naval Ship Research and Development Center, report NSRADC 417-H01, 1971.

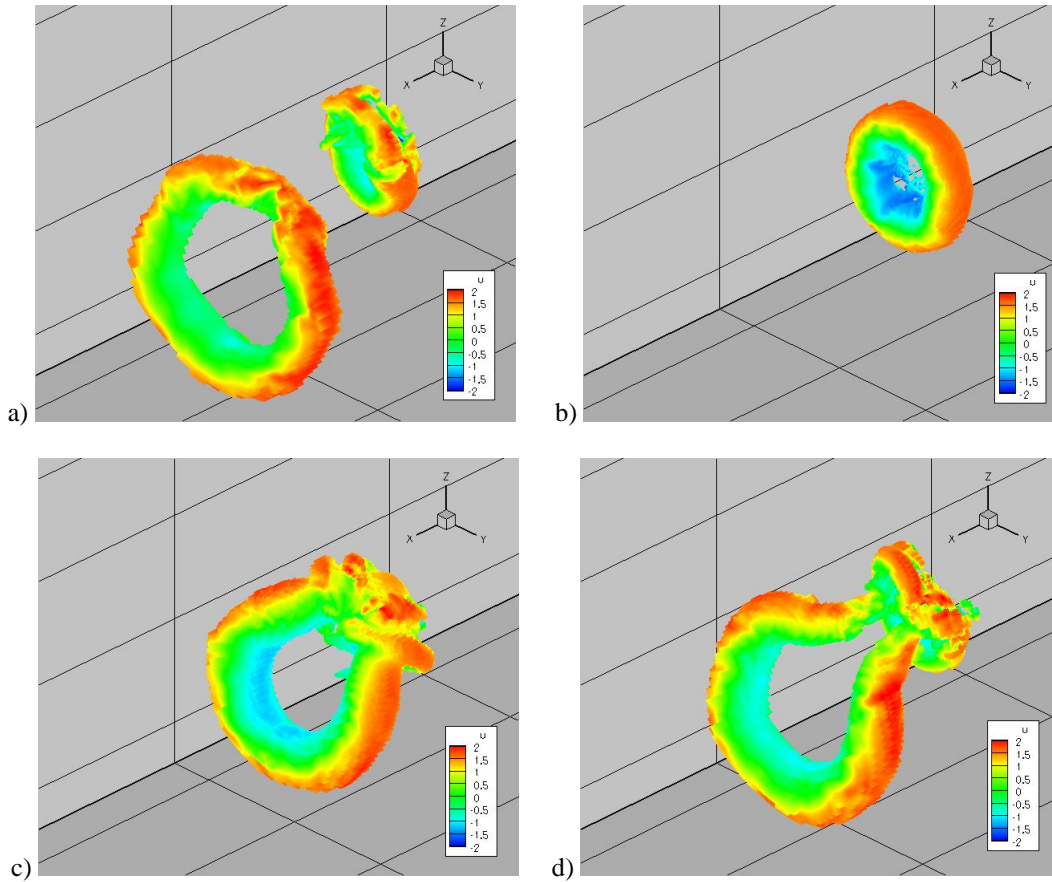


Figure 4: Time evolution of the ring vortex for actuator disk with $U_p/U=-1$, $Re=1200$. Colors show axial velocity at an isosurface of low pressure in a 3-D view. Free stream flow is in positive x-direction, i.e. from right top to left bottom corner; the actuator disk is not plotted.

In sequence:

- (a) shows a new ring vortex (right) created around the actuator disk while the old ring vortex (left) drifts away, (b) shows growth of the ring vortex, (c) ring vortex is stretched downstream, (d) ring vortex is shed, while a new one appears.**

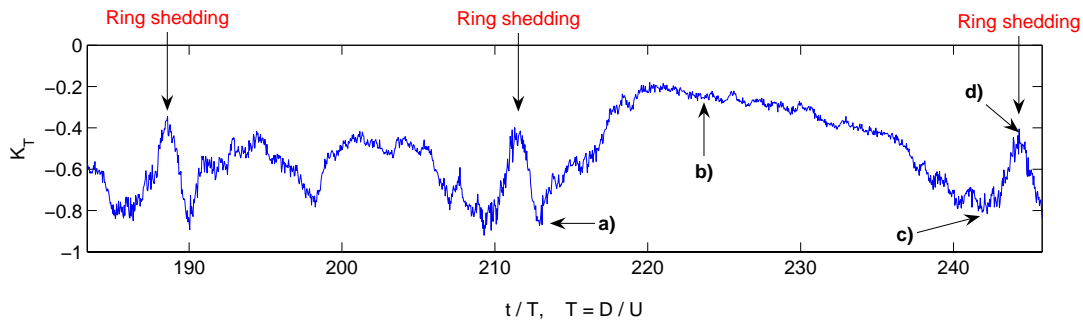


Figure 5: Time evolution of non-dimensional thrust K_T for actuator disk with $U_p/U=-1$, $Re=1200$. The labels a, b, c, d show times corresponding to plots a, b, c, d of Figure 4.

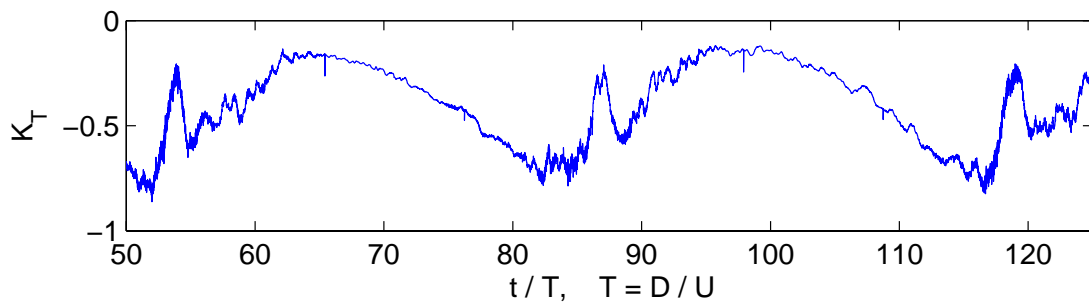


Figure 6: Time evolution of non-dimensional thrust K_T for actuator disk with $U_p/U=-1$, $Re=1200$ computed on a fine grid (13 million control volumes).

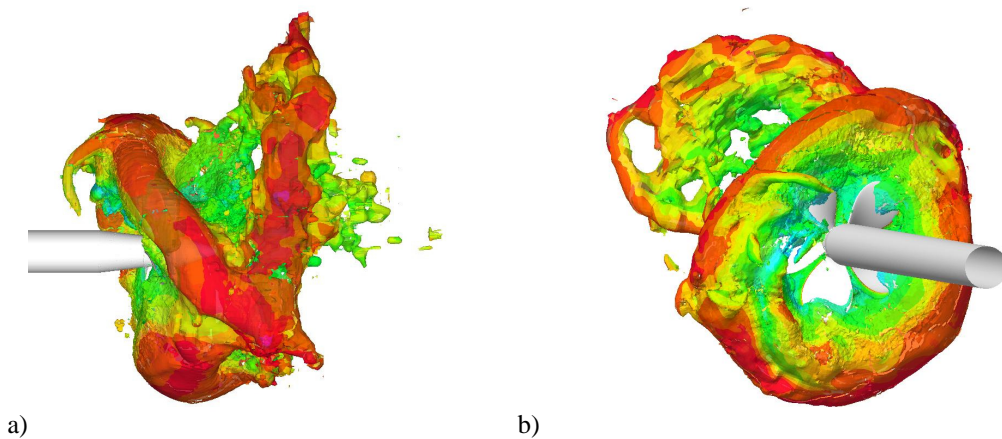


Figure 7: Results computed for real propeller geometry⁶ at $J = -0.7$, $Re = 480,000$. Colors show axial velocity at an isosurface of low pressure in a 3-D view. (a) side view (b) view from upstream.